EXPERIMENTAL DETERMINATION OF THE RESIDUAL STRESSES IN A KRAFT RECOVERY BOILER TUBE

Xun-Li Wang, E. Andrew Payzant, Bostjan Taljat, Camden R. Hubbard, James R. Keiser
Metals and Ceramics Division
Oak Ridge National Laboratory
PO Box 2008, Oak Ridge, TN, 37831-6064

ABSTRACT

Neutron diffraction was used to determine the residual stresses in a spiral weld overlay tube used in Kraft recovery boilers by the pulp and paper industry. The specimen was a 2.5" OD carbon steel tube covered with a layer of Inconel 625 weld overlay. Residual strains in the carbon steel and weld overlay layers were determined using the ferritic (211) and austenitic (311) reflections, respectively. Residual stresses in each material were derived from the measured strains using Hooke's law and appropriate elastic constants. Tensile stress regions were found not only in the weld metal but also in the heat affected zone in the carbon steel. The maximum tensile stress was located in the weld overlay layer and was found to be 360 MPa, or about 75% of the yield strength of the weld metal. The experimental data were compared with a finite element analysis based on an uncoupled thermal-mechanical formulation. Overall, the modeling results were in satisfactory agreement with the experimental data, although the hoop strain (stress) appears to have been overestimated by the finite element model. Additional neutron diffraction measurements on an annealed tube confirmed that these welding residual stresses were eliminated after annealing at 900°C for 20 minutes.

1. INTRODUCTION

Black liquor recovery boilers are a critical component in Kraft pulp mills [Keiser 1996, Singbeil 1996]. They provide a means for the mills to recover chemicals used in the pulping process and to produce process steam which generates a significant portion of the electricity required for mill operation. Metal tubes are an essential part of a recovery boiler comprising the floor, walls, roof and the superheater. Much of the metal tubing is carbon steel, but because the boiler atmosphere is quite corrosive, composite tubing of stainless steel on carbon steel is commonly used in some areas to provide additional corrosion resistance.

While the use of composite tubes has solved most of the corrosion problems experienced by carbon steel tubes, significant cracking has been reported [Singbeil 1996] in the stainless steel layer of composite tubes subjected to service. Metallographic examination indicates that the cracks always initiate at the outer surface and penetrate radially through the stainless steel layer. Nearly always, the cracks stop at or before reaching the interface between the carbon steel and stainless steel layers. However, there are also cases where the cracks propagate along the interface, impeding heat transfer and producing a crevice where corrodants can be trapped. In a few cases, delamination and spalling of chunks of the stainless steel layer have occurred, resulting in the exposure of the carbon steel core to the boiler atmosphere. The mechanism of cracking is currently the subject of a multi-disciplinary study [Keiser 1996]. Alternate cladding materials, including nickel-based alloys, are being considered.

Composite tubes are typically made by co-extrusion at elevated temperatures, followed by cold reduction, annealing, and straightening. Recently, there has been growing interest in an alternative manufacturing technology, where the corrosion resistant layer is applied to the carbon steel tube by welding. Limited experience to date [Singbeil 1996] with boilers containing tubes covered with weld overlay shows less frequent occurrence of cracking. In addition, because of the metallurgical bonding between the weld metal and the carbon steel, weld overlay tubes are expected to exhibit better adhesion characteristics, reducing the possibility of crack propagation along the interface. This welding process can be automated to yield large output at a reduced cost and therefore has attracted special attention.

A fundamental issue associated with weld overlay tubes is that large tensile residual stresses are present due to thermal shrinkage of the weld metal following the deposition. The tensile residual stresses in the weld layer could cause degradation by stress-corrosion cracking and contribute to thermal fatigue when the tubes are subjected to thermal cycling. Thus, there is a critical need to quantify these residual stresses and look for ways to minimize them. In this paper, we describe a neutron diffraction measurement of the residual stresses in a spiral weld overlay tube. To assess the effect of heat treatment on residual stresses, a tube annealed at 900°C was also measured.

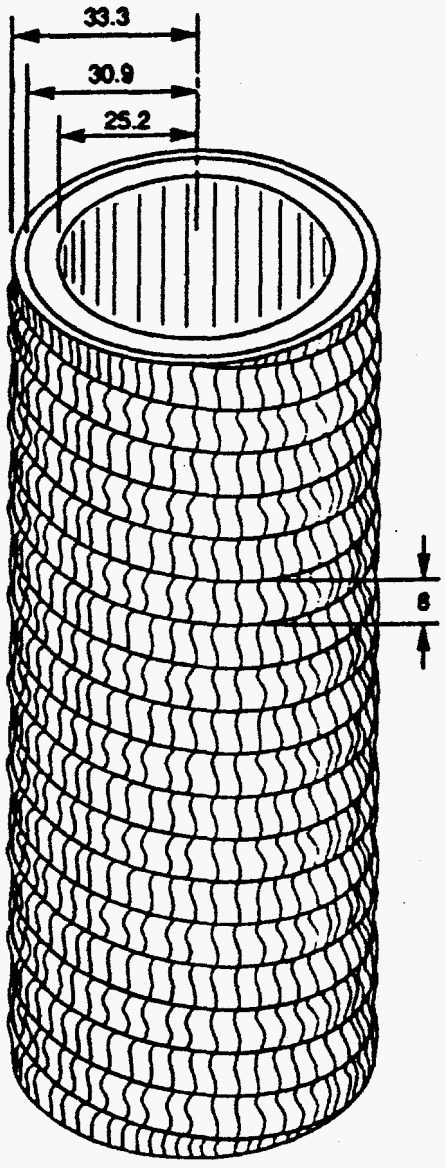

Fig. 1. Schematic of the weld overlay tube specimen.

2. EXPERIMENTAL PROCEDURES

2.1 Sample Preparation and Microstructure

The spiral weld overlay tubes were fabricated by Welding Services, Inc., Norcross, Georgia. The core material was SA-210 carbon steel and the weld metal was alloy 625, a nickel-based alloy. The welding process consisted of two steps. First a layer of 625 filler material was deposited in the circumferential direction using an automated Gas Metal Arc Welding (GMAW) process. Then an automated Gas Tungsten Arc Welding (GTAW) process was utilized, but with no filler material. The tube was water cooled throughout the entire welding process and no preheat was applied. The finished product was approximately 10 ft. long, and a section of it was used for residual stress analysis. The specimen length (approximately 4× diameter) was chosen so that the relaxation of residual stresses due to segmentation was negligible at mid-length. Fig. 1 shows a schematic of the specimen. To assess the effect of stress relief via heat treatment, a similarly prepared specimen was annealed at 900°C for 20 min., air-cooled, and measured with neutron diffraction. Unless specified otherwise, all data presented refer to the as-welded tube.

Fig. 2 is a photomicrograph showing a cross-section of the weld overlay tube under study. The interface between the carbon steel core and the weld overlay layer is easily discerned from the micrograph. The interface is not quite uniform, presumably because of various degrees of penetration by the weld metal. The weld overlay layer has the expected dendritic structure with large grains (some greater than 100 μm), whereas the carbon steel is fine grained. The micrograph also reveals the heat affected zone, which extends about 1.5 mm into the carbon steel core. The annealed specimen shows similar microstructure for the weld layer. The dendritic structure still exists and there is little change in grain size. The carbon steel layer, on the other hand, shows a slight reduction in grain size, indicating recrystallization of the carbon steel during annealing. This is consistent with the annealing temperature (760°C [Smith 1970, ASM 1989]) of SA-210 carbon steel. The annealing temperature of alloy 625 is higher (980°C [ASM 1992]) than the heat treatment temperature, thus no change in microstructure is expected. In that sense, at 900°C only the carbon steel layer of the tube was fully annealed.

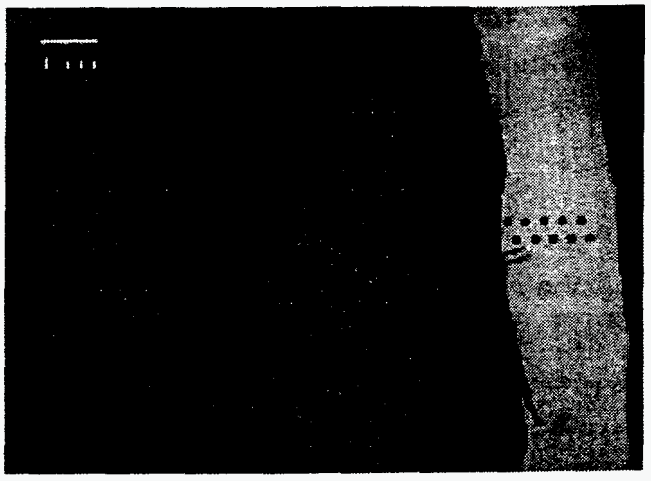

Fig. 2. Photomicrograph showing the interface of the weld overlay tube

2.2 Neutron Diffraction Measurements

The principle of residual stress determination using neutron diffraction has been described previously by several authors [Krawitz 1990, Wang 1996, Webster 1996]. In this method, one measures the angular position of one or more diffraction peaks,

from which the interplanar lattice spacing is determined using Bragg's law,

$$\lambda = 2d \sin\theta \qquad (1)$$

where λ is the neutron wavelength, d and 2θ are, respectively, the lattice spacing and diffraction angle of the reflection of interest. The lattice strain is then obtained using the equation,

$$\varepsilon = \frac{d - d_0}{d_0} \qquad (2)$$

where d_0 is the unstressed lattice spacing. Small bars of 5 mm width cut from SA-210 and alloy 625 were used as stress-free reference specimens. For a given specimen orientation, the strain component parallel to the scattering vector is measured. From the measured residual strains, residual stresses are derived using Hooke's law and appropriate elastic constants.

The neutron diffraction measurements were conducted at the High Flux Isotope Reactor of Oak Ridge National Laboratory. Details of the instrument have been given previously [Wang 1996]. In the present experiment, a Be (11.0) monochromator reflection was used with a take-off angle of 84°, giving an incident neutron wavelength of 1.513 Å. Neutron diffraction peak profiles were recorded with a position-sensitive-detector. For measurements of the radial and hoop strains (ε_{rr} and $\varepsilon_{\theta\theta}$), the tube axis was mounted upright, and slits of dimensions 0.8mm × 30mm were inserted before and after the specimen, which together defined a sampling volume of 19.2 mm^3. For measurements of the axial strain (ε_{zz}), the tube axis was mounted horizontally. Slits of dimensions 1mm × 4mm and 1mm × 30 mm were used in this case, and the sampling volume thus defined was 4 mm^3. Strain mapping was accomplished using a three-dimensional translation stage mounted on the sample table of the neutron diffractometer.

For the carbon steel core, the body-centered cubic (2 1 1) reflection was used for strain determination. For the weld overlay layer, the face-centered cubic (3 1 1) reflection was measured. With the current experimental setup, the nominal diffraction angles for these two reflections were 80.9° and 88.8°, respectively. Each recorded diffraction profile was fitted to a Gaussian function to yield the position, width, and intensity of the peak.

To ensure that the obtained strain values were representative, the radial strain profile was determined at four angular locations (90° apart). Since hoop strain data took longer to collect due to the unfavorable beam path in this measurement geometry, the hoop strain profile was determined at two angular positions 180° apart. Checks were also made around the tube at a given radial position from the interface in both the carbon steel core and the weld overlay layer. ε_{zz} was measured at only one angular position, because of the small sampling volume and hence long counting time required for this measurement geometry.

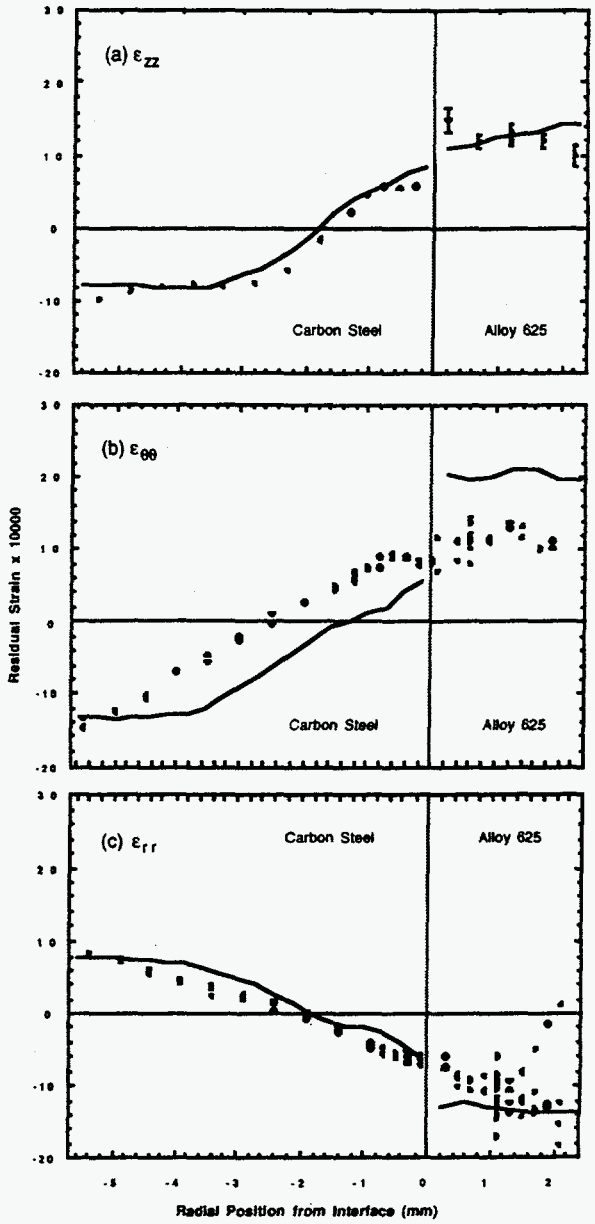

Fig. 3. Experimentally determined residual strains as a function of the radial position from the interface. The solid lines are calculations from a finite element analysis.

3. EXPERIMENTAL RESULTS

The experimentally determined residual strains are shown in Fig. 3. Radial strain data in the vicinity of the interface and outer surface were corrected for an artificial peak shift resulting from

partial burial of the sampling volume using a Monte Carlo computer program [Spooner 1997]. The maximum correction was 0.045°, or 4×10^{-4} in strain. Hoop and axial strain data were not corrected, since in these experimental configurations the anticipated peak shift artifact was not significant (≤0.01°).

Note that in Fig. 3, all data points obtained at different angular positions are plotted together. It can be seen that at a given radial position, strains in the carbon steel vary little from one angular position to another. On the other hand, strains in the weld overlay show significant scatter as a function of the angular position. To illustrate this point, Fig. 4 shows the hoop strain data obtained at 0.7 and 1.0 mm from the interface in the carbon steel and weld overlay, respectively. The observed integrated intensities also show similar angular dependence: almost constant in the carbon steel and scattered in the weld overlay layer. These observations suggest that cylindrical symmetry holds for this weld overlay tube; the scatter in the weld overlay layer is attributable to the presence of large grains resulting from the solidification of the weld deposit, as shown by metallography, and possibly some deviation from true cylindrical symmetry due to the helical symmetry of the weld overlay.

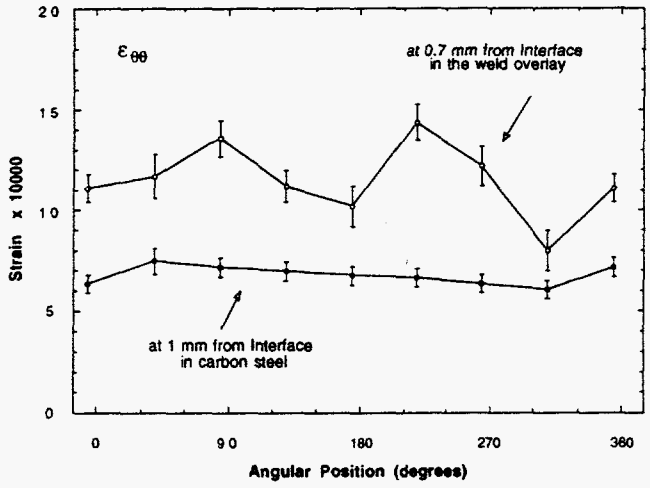

Fig. 4 Hoop strain data as a function of the angular position at 0.7 mm and 1.0 mm from the interface in the carbon steel and weld overlay layers, respectively.

The residual stresses in each material were derived from the measured strains using the following diffraction elastic constants: E=210 GPa and ν=0.28 for the (211) reflection of carbon steel [Pintshovius 1986], and E=184 GPa and ν=0.29 for the (311) reflection of alloy 625 [ASM 1992, Webster 1995]. Except for ε_{zz}, which was measured at only one angular position, average strain values over all angular positions were used for calculation of residual stresses. The final results are shown in Fig. 5. The experimental uncertainty of the stress values was estimated to be ±25 MPa in the carbon steel core and ±50 MPa in the weld overlay layer. Because a correction had to be made for the radial strain data near the interface and outer surface, the uncertainty in these regions is greater.

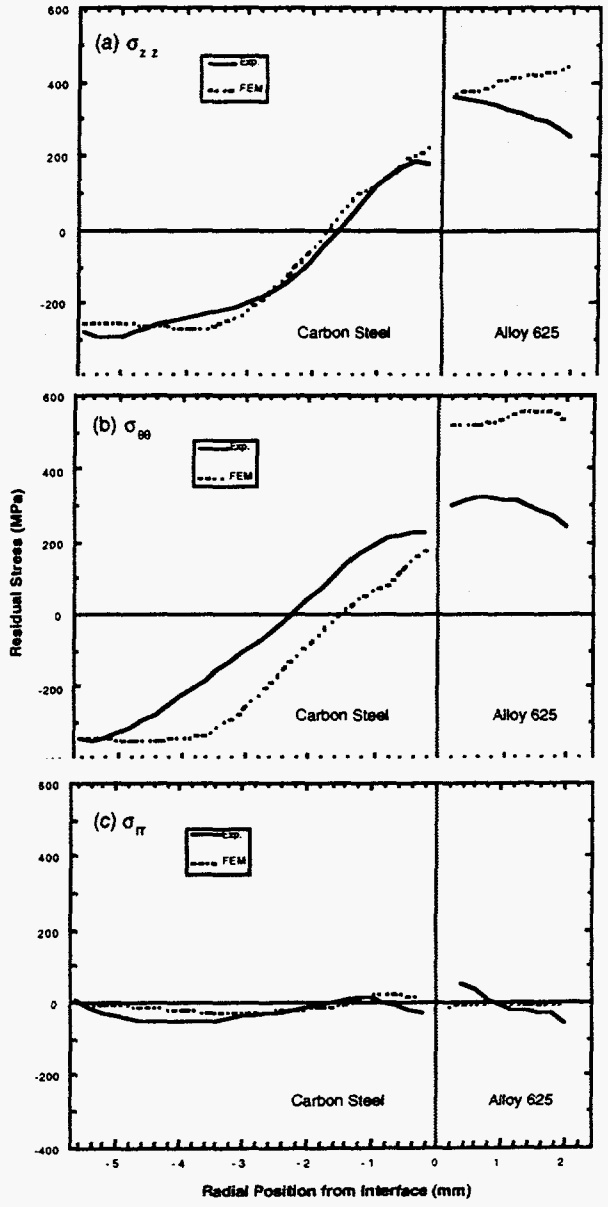

Fig. 5 Residual stresses in the weld overlay tube. The dashed lines are calculations from a finite element analysis.

It is seen that σ_{zz} and $\sigma_{\theta\theta}$ are tensile over the entire thickness of the weld overlay layer, which is a direct consequence of thermal shrinkage of the weld metal during cooling following solidification. The maximum tensile stress is approximately 360 MPa. σ_{zz} and $\sigma_{\theta\theta}$ in the carbon steel, on the other hand, vary from compressive near the inner radius to tensile near the interface, and range between -350 and 220 MPa. σ_{rr} is low throughout the weld overlay tube, as it should be because of the small wall thickness compared to the diameter of the tube.

Fig. 6 shows that the hoop strain data ($\varepsilon_{\theta\theta}$) obtained for the as-welded tube was reduced to almost zero following the annealing procedure. Similar degrees of reductions were also observed in ε_{zz} and ε_{rr} obtained for the carbon steel core. This means that the residual stresses vanish in the carbon steel after annealing. Attempts were made to determine ε_{zz} and ε_{rr} in the weld overlay layer as well. However, it proved difficult to obtain good intensity for many of the measurement locations in the weld overlay layer. These observations can be attributed to the presence of a strong crystallographic texture and/or large grain sizes in the weld overlay layer of this particular specimen. From the strain values in the carbon steel and considering the conditions of static equilibrium, it can be inferred that the residual stresses in the weld overlay must be very close to zero as well. The hoop strain data in the weld overlay layer (Fig. 6) support this conclusion.

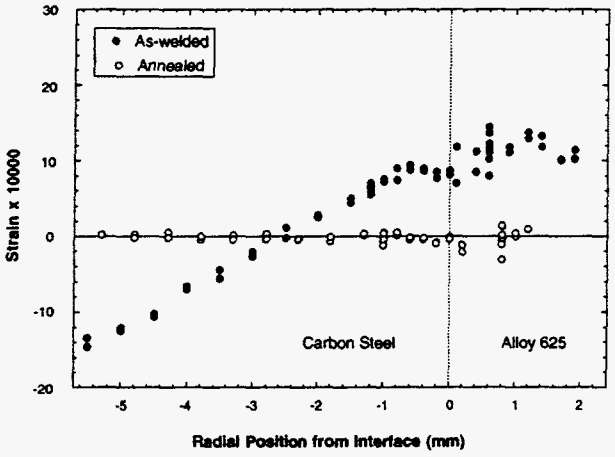

Fig. 6 Comparison of the hoop strain profile obtained in the as-welded and annealed tube.

4. DISCUSSION

The residual stress data obtained for the as-welded tube can be checked against the equations of static equilibrium and the boundary conditions. For specimens having cylindrical symmetry, the following equations representing the state of static equilibrium should hold [Pintshovius 1986, Noyan 1987],

$$\int \sigma_{zz} r dr = 0 \tag{3}$$

$$\int \sigma_{\theta\theta} dr = 0 \tag{4}$$

$$\int \frac{\sigma_{rr} - \sigma_{\theta\theta}}{r} dr = 0 \tag{5}$$

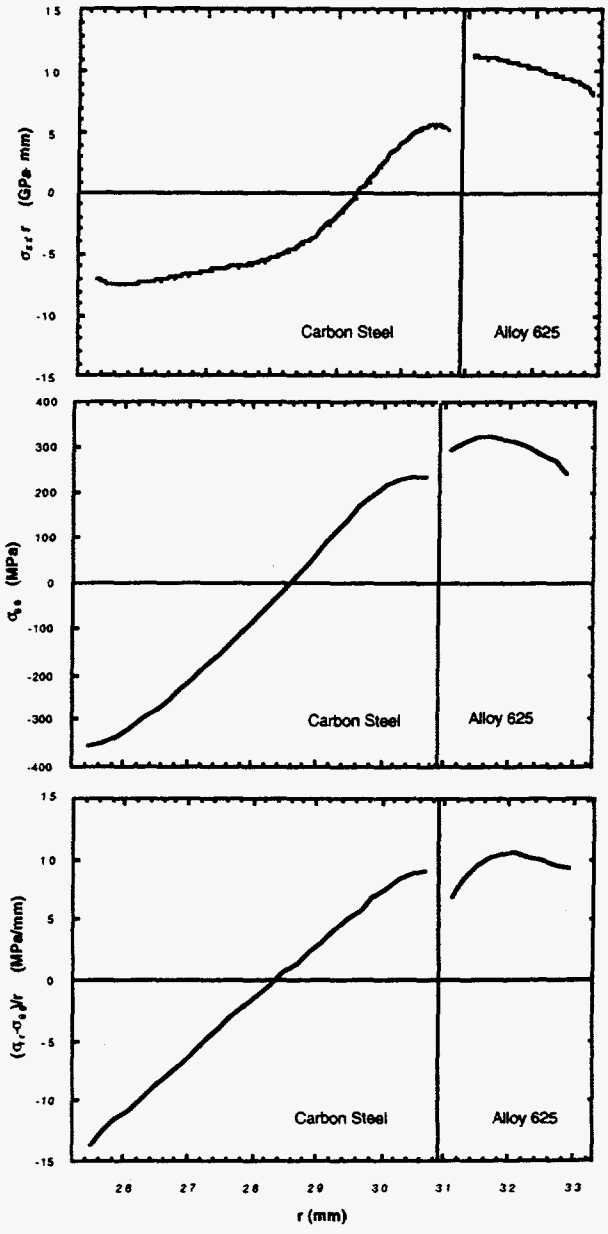

Fig. 7. Quantities of (a) σ_{zz}·r, (b) $\sigma_{\theta\theta}$, and (c) $(\sigma_{\theta\theta}-\sigma_{rr})/r$ calculated from the stress values shown in Fig. 5. In a specimen exhibiting cylindrical symmetry, the integral of these quantities over the wall thickness should be zero.

The integration takes place from the inner radius to the outer radius. In Fig. 7, σ_{zz}·r, $\sigma_{\theta\theta}$, and $(\sigma_{\theta\theta}-\sigma_{rr})/r$ are plotted as a function of *r*. From Fig. 7 it can be seen that Eqs. (3-5) are satisfied to within the experimental precision. This result also corroborates that the tube specimen under study has cylindrical symmetry. The boundary conditions require that σ_{rr} disappear at the inner and outer surfaces and continue across the interface. As shown by Fig. 5(c), these conditions are also satisfied to within the experimental precision. As a final check, the experimental stress values were balanced using a tube cross-sectional finite element model [Taljat 1997]. The results of this analysis further confirm that the experimental stress values shown in Fig. 5 satisfy very well the equations of static equilibrium and the boundary conditions.

Note that σ_{zz} and $\sigma_{\theta\theta}$ are tensile not only in the weld overlay layer, but also in the carbon steel adjacent to the interface. Compressive residual stresses are seen only in regions well inside the interface. These observations are similar to those observed in a weld overlay applied to a flat plate [Feng 1996] and are attributable to the through-thickness temperature gradients during cooling of the weld deposit. The scope of the tensile stress region in the carbon steel core appears to be consistent with the heat affected zone revealed by the photomicrograph [Fig. 2].

The maximum tensile residual stresses are 220 and 360 MPa, respectively, in the carbon steel and weld overlay layer. Both values amount to 70-75% of the 0.2% yield strength for each material, which are 300 and 510 MPa [Smith 1970, ASM 1989, ASM 1992], respectively, at room temperature. The maximum compressive stresses are approximately 350 MPa in the carbon steel near the inner radius. These values are slightly higher than the 0.2% yield strength of the carbon steel, but the difference is within twice the experimental precision.

The large residual stresses in the weld overlay could potentially pose a serious problem for applications of weld overlay tubes as corrosion-resistant materials. Fortunately, as Fig. 6 illustrated, the residual stresses in as-welded overlay tubes can be reduced to almost zero by heat-treatment at 900°C.

In order to gain insight into the thermal-mechanical process following the weld deposition, a finite element analysis was conducted in parallel with the neutron diffraction work. The analysis can be used to calculate, among other quantities, residual stresses in as-welded tubes, although the eventual goal is to evaluate the temperature effects on residual stresses when the tubes are placed under service conditions. The analysis used an uncoupled approach, i.e., the thermal analysis was performed first and then, based on the calculated temperature history, the mechanical state (including residual stresses) was calculated. An axisymmetric model was assumed, which greatly simplified the modeling efforts and facilitated the calculations. The materials properties used in the calculations were taken from the literature [Smith 1970, ASM 1989, ASM 1992]. Other aspects of the finite element model are reported and discussed elsewhere [Taljat 1997].

The calculated residual strains and stresses are also plotted in Fig. 3 and Fig. 5, so that a comparison can be made with the experimental results. Trendwise, the model reproduces very well the spatial dependence of the experimental data. Even on a quantitative basis, the calculated ε_{zz} and ε_{rr} are also in agreement with the experimental values. The same is true for the calculated σ_{zz} and σ_{rr}. However, for the $\varepsilon_{\theta\theta}$ and $\sigma_{\theta\theta}$, the model seems to have consistently overestimated the experimental values.

One possibility for the differences seen here is that the materials properties used in the finite element model were not very accurate. In fact, calculations made with a lower yield strength weld metal showed better agreement with the experimental data. Also, the present model ignored possible mixing between the carbon steel and weld metal in the vicinity of the interface. This gives rise to the marked difference in $\varepsilon_{\theta\theta}$ and ε_{rr} across the interface. The measured $\varepsilon_{\theta\theta}$ and ε_{rr} (Fig. 3), on the other hand, show far less difference than predicted, suggesting that on a microscopic scale, the interface is not sharply defined. This could be due to the wavy nature of the interface, as shown in Fig. 2, or some degrees of mixing between the weld metal and the carbon steel, giving gradually varying materials properties across the interface.

The finite element analysis indicates that the entire weld overlay layer plus part of the carbon steel yielded during cooling. Indeed, the measured diffraction peak width shows considerable broadening throughout the weld overlay layer and in the heat-affected zone of the carbon steel, which are indications of plastic yielding in these regions. The plateaus exhibited by σ_{zz} and σ_{rr} in the carbon steel adjacent to the interface provide additional evidence of yielding [Pintshovius 1994].

The overall agreement between the experimental data and calculations demonstrates that essential features of the thermal-mechanical process following the weld deposition are covered in the present finite element model. Consequently, other modeling results may be discussed with reasonable confidence [Taljat 1997].

Finally, a note can be made on the nearly zero residual strains observed in the annealed tube. Normally, post-weld heat treatment relaxes only the welding residual stresses. Upon uniform cooling from the heat-treatment temperature, another type of residual stress could develop due to the thermal expansion mismatch between the base materials and the weld metal. In the weld overlay tubes under study, the coefficient of thermal expansion of alloy 625 is almost identical to that of carbon steel (12.1×10^{-6} K^{-1} vs. 12.8×10^{-6} K^{-1} [Smith 1970, ASM 1989, ASM 1992]). This explains why the weld overlay tubes remain stress-free after cooling from the annealing temperature.

5. SUMMARY

In this study, residual stresses in a spiral weld overlay tube were determined by means of neutron diffraction. The residual stress data are of high quality in that they satisfy the conditions of static equilibrium and the boundary conditions. Although significant plastic yielding took place during cooling, considerable tensile stresses were found to exist in the weld overlay layer as well as in the heat affected zone in the carbon steel. However, these residual stresses can be eliminated by annealing 900°C for 20 min. The experimental data shown here provide a necessary check of the finite element model currently being developed for modeling the residual stresses in weld overlay tubes under service conditions.

ACKNOWLEDGEMENTS

Research sponsored by the Assistant Secretary for Energy Efficiency and Renewable Energy, Office of Industrial Technologies, as part of the Advanced Industrial Materials Program. The HFIR neutron facility is sponsored by the Assistant Secretary for Energy Research through the Office of Basic Energy Sciences. Oak Ridge National Laboratory is managed by Lockheed Martin Energy Research Corp. for the US Department of Energy, under contract DE-AC05-96OR22464. EAP was supported by an appointment to the ORNL Postdoctoral Research Associates Program administered jointly by ORNL and ORISE.

REFERENCES

Alan, A. J., Hutchings, M. T., Windsor, C. G., and Andreani, C., 1985, *Adv. Phys.*, **34**, 445-473.

ASM, 1989, *High Temperature Property Data*, ASM International, Metals Park, Ohio.

ASM, 1992, *Materials Handbook*, Desk Edition, ASM International, Metals Park, Ohio,.

Feng, Z., Wang, X.-L., Spooner, S., Goodwin, G. M., Masiasz, P. J., Hubbard, C. R., and Zacharia, T., 1996, *Proc. of 1996 ASME Pressure Vessels and Piping Conference*, PVP-Vol **327**, 119-126.

Keiser, J. R., Taljat, B., Wang, X.-L., Masiasz, P. J., Hubbard, C. R., Swindeman, R.W., Singbeil, D.L., and Prescott, R., 1996, to appear in *Proc. of 1996 TAPPI Engineering Conf.*

Krawitz, A. D. and Holden, T. M., 1990, *MRS Bulletin*, November, 57-64.

Noyan, I. C., and Cohen, J. B., 1987, *Residual Stress - Measurement by Diffraction and Interpretation*, Springer-Verlag, New York, p.218.

Singbeil, D.L., Prescott, R., Keiser, J. R., and Swindeman, R.W., 1996, *draft technical report*, Pulp and Paper Research Institute of Canada.

Smith, G. V., 1970, *An Evaluation of the Elevated Temperature Tensile and Creep-Rupture Properties of Wrought Carbon Steel*, ASTM, Philadelphia.

Pintschovius, L., Jung, V., Macherauch, E., and Vohringer, O., 1983, *Mat. Sci. Eng.*, **61**, 43-50.

Pintschovius, L., Macherauch, E., and Scholtes, B., 1986, *Mat. Sci. Eng.*, **84**, 163-170.

Pintschovius, L., Pyka, N., Kubmaul, R., Munz, D., Eigenmann, B., and Scholtes, B., 1994, *Mat. Sci. Eng.*, **A177**, 55-61.

Spooner, S. and Wang, X.-L., 1997, *J. Appl. Cryst.*, in the press

Taljat, B. et al., 1997, to be published.

Wang, X.-L., Spooner, S., Hubbard, C. R., Goodwin, G. M., Masiasz, P. J., Feng, Z., and Zacharia, T., 1995, *Mat. Res. Soc. Symp. Proc.*, **364**, 109-114.

Wang, X.-L., Hubbard, C. R., Spooner, S., David, S. A., Rabin, B. H., and Williamson, R. L., 1996, *Mat. Sci. Eng.*, **A211**, 45-53.

Webster, P. J., Mills, G., Wang, X. D., Kang, W. P., and Holden, T. M., 1995, *J. Strain Analysis*, **30**, 35-43.

Webster, P. J., Mills, G., Wang, X. D., Kang, W. P., and Holden, T. M., 1996, *J. Neutron Res.*, **3**, 223.